Available online at www.sciencedirect.com
SCIENCE DIRECT
Experimental Eye Research 82 (2006) 935–944
EXPERIMENTAL EYE RESEARCH
www.elsevier.com/locate/yexer

Caldesmon transgene expression disrupts focal adhesions in HTM cells and increases outflow facility in organ-cultured human and monkey anterior segments

B'Ann True Gabelt [a,*], Yujie Hu [a], Jason L. Vittitow [b], Carol R. Rasmussen [a], Inna Grosheva [c], Alexander D. Bershadsky [c], Benjamin Geiger [c], Terete Borrás [b], Paul L. Kaufman [a]

[a] Department of Ophthalmology and Visual Sciences, University of Wisconsin, Madison, WI 53792, USA
[b] Department of Ophthalmology, University of North Carolina, 6109 NeuroSci Res Bldg, Box 7041, Chapel Hill, NC 27599, USA
[c] Department of Molecular Cell Biology, Weizmann Institute of Science, Rehovot 76100, Israel

Received 29 August 2005; accepted in revised form 9 December 2005
Available online 26 January 2006

Abstract

Cytoskeleton modulating compounds have been shown to lower intraocular pressure (IOP) and increase outflow facility. Caldesmon is one protein that is involved in the regulation of actin stress fiber formation. The effects of rat non-muscle caldesmon (Cald) gene over-expression on focal adhesions in human trabecular meshwork (HTM) cells and on outflow facility in organ-cultured human and monkey anterior segments were determined. Treatment of HTM cells with adenovirus-delivered caldesmon (AdCaldGFP) resulted in characteristic changes in the actin cytoskeleton and matrix adhesions within 24–48 hr post-transduction. Stress fibers gradually disappeared and novel actin structures were formed (see manuscript by Grosheva et al., this issue). In cells with disrupted stress fibers, vinculin-containing focal adhesions were also disrupted. In organ-cultured anterior segments, baseline outflow facility ($\mu l\ min^{-1}\ mmHg^{-1}$) for all anterior segments averaged (mean $\pm$ SEM): human, 0.19 ± 0.03 ($n=12$); monkey, 0.36 ± 0.02 ($n=19$). In human anterior segments, transduction with 10^7 plaque forming units of AdGFPCald increased outflow facility by $43 \pm 21\%$ ($p \leq 0.11$, $n=6$) at 66 hr compared to baseline and corrected for the changes in outflow facility of the contralateral vehicle treated segment. Using the same time point, i.e. 2–3 days after injection, outflow facility in monkey anterior segments, transduced with 1.5×10^7 plaque forming units of AdGFPCald was increased by $35 \pm 18\%$, $p<0.2$, $n=10$ compared to baseline and corrected for the change in outflow facility in the contralateral AdGFP treated segment. Combining human (66 hr) and monkey (2–3 days) data, outflow facility was increased by $38 \pm 13\%$, $p<0.02$, $n=16$. Additional analysis of maximum responses in monkey anterior segments from 1 to 6 days after transduction showed outflow facility was increased by $66 \pm 18\%$, $p<0.01$, $n=10$. Caldesmon over-expression, which relaxes cultured HTM cells and disrupts their actin cytoskeleton and cell–matrix adhesions, also appears to increase outflow facility in organ-cultured human and monkey anterior segments. This suggests that over-expression of the caldesmon gene in the TM may be an effective approach for the gene therapy of glaucoma.

Keywords: actin cytoskeleton; caldesmon; focal adhesions; gene therapy; outflow facility; organ-cultured anterior segments; trabecular meshwork; vinculin

1. Introduction

Present pharmacotherapy of glaucoma involves lowering intraocular pressure (IOP). This is accomplished by frequent repetitive administration of exogenous molecules to enhance aqueous humour outflow or reduce its inflow (Ritch et al., 1996). Modern molecular genetic technology raises the possibility of bypassing the external agent and 'setting' the inflow or outflow tissues to a different 'performance' level genetically. This would have the great advantage of eliminating the need for repetitive drug application by the patient (Goldberg, 1999).

Cytoskeleton modulating compounds have been shown to lower IOP and/or enhance outflow facility in vivo and/or in vitro (review in, Epstein et al., 1999; Kaufman et al., 2000).

* Corresponding author. B'Ann True Gabelt, Department of Ophthalmology and Visual Sciences, University of Wisconsin, 600 Highland Ave, F4/340 CSC, Madison, WI 53972, USA.
E-mail addresses: btgabelt@wisc.edu (B.T. Gabelt), yujiehu@wisc.edu (Y. Hu), jvittitow@inspirepharm.com (J.L. Vittitow), crasmussen@wisc.edu (C.R. Rasmussen), inna.grosheva@weizmann.ac.il (I. Grosheva), alexander.bershadsky@weizmann.ac.il (A.D. Bershadsky), benny.geiger@weizmann.ac.il (B. Geiger), tborras@med.unc.edu (T. Borrás), kaufmanp@mhub.ophth.wisc.edu (P.L. Kaufman).

0014-4835/$ - see front matter © 2006 Elsevier Ltd. All rights reserved.
doi:10.1016/j.exer.2005.12.002

Cell contractility is a major factor controlling the formation of stress fibers and focal adhesions. Experiments with various inhibitors, including H-7, KT-5926, ML-7, BDM, Y-27632, and dominant negative RhoA, that affect different pathways of myosin II regulation revealed a strong correlation between suppression of myosin II-driven contractility and impaired formation of stress fibers and associated focal contacts (Volberg et al., 1994; Bershadsky et al., 1996; Chrzanowska-Wodnicka and Burridge, 1996; Pelham and Wang, 1997; Riveline et al., 2001). These inhibitors have also been shown to either lower IOP and/or increase outflow facility in vitro and/or in vivo (Tian et al., 1998; Epstein et al., 1999; Tian et al., 2000; Honjo et al., 2001; Rao et al., 2001; Vittitow et al., 2002; Bahler et al., 2004; Tian et al., 2004). H-7 and latrunculin-induced increases in outflow facility result from major morphological and architectural changes in the TM, including apparent cell relaxation, expansion of the juxtacanalicular region, dilation of Schlemm's canal and luminal protrusion of the inner wall cells (Sabanay et al., 2000, 2004). Based on these data, it was anticipated that over-expression of cytoskeleton-relaxing proteins in the TM may be considered as novel gene therapies for glaucoma.

One such candidate protein is caldesmon, which, in smooth muscle cells, is involved in the regulation of myosin II activity by blocking its interaction with actin (reviewed in, Huber, 1997; Chalovich et al., 1998; Marston et al., 1998). The properties of non-muscle caldesmon (the form present in the trabecular outflow pathway) are quite similar (reviewed in, Matsumura and Yamashiro, 1993; Huber, 1997).

Caldesmon over-expression in cells was directly demonstrated to lead to suppression of cellular contractility in cultured cells, manifested by a reduced capacity to develop traction forces applied to the underlying extracellular matrix (Helfman et al., 1999). This relaxation of the cells resembles, in many ways, the effect of H-7 on the contractility of cells. In particular, over-expression of caldesmon in cultured cells (Helfman et al., 1999) leads to the loss of stress fibers and focal adhesions. It is important that caldesmon over-expression prevents focal adhesion and stress fiber formation even if the cells express constitutively active Rho, showing that caldesmon is operating downstream from the Rho signalling pathway.

In a separate paper in this issue, the effects of caldesmon over-expression on the actin cytoskeleton of cultured HTM cells is presented. In the current study, we report the effects of adenovirus-mediated caldesmon delivery on focal adhesions in HTM cells and on outflow facility in organ-cultured human and monkey anterior segments. This study further supports the potential of gene therapy based approaches in the treatment of glaucoma.

2. Materials and methods

2.1. Recombinant replication deficient adenoviral (Ad) vector carrying rat Caldesmon (Cald) and GFP genes

AdGFPCald, was generated by overlap recombination (Fig. 1). The expression cassette of this recombinant virus contains a fusion of the green fluorescent protein (GFP) cDNA (nucleotides (nt) 284–1001 in GenBank accession no. U76561) with the coding region of the rat caldesmon cDNA (nt 724–2319 in GenBank accession no. NM013146). The expression cassette was obtained by PCR amplification of plasmid pGFPCald (Helfman et al., 1999) using forward 5′-AGCTGTTTAAACCACCATGGTGAGCAAGGGCGAG GAGCT-3′ (284–311 nt GFP cDNA) and reverse 5′-ATGCG-GATCCTCAGACCTTAGTGGGAGAAGT-3′ (2318–2299 nt rat caldesmon cDNA) primers. The total length of the cassette is 2323 nt. The forward primer contains 4 extra nt in its 5′ plus a Pme I restriction site. This primer introduces the GFP natural Kozack sequences into the cassette and allows initiation of translation at the GFP ATG initiation codon. The reverse primer contains four extra nt in its 5′ plus a Bam HI restriction site. The amplified insert was cloned into the pCR 2.1 vector (Invitrogen, San Diego, CA) (pJV10). The pJV10 insert was isolated by digestion with Pme I-Bam HI and sub cloned into the shuttle vector pQBI-AdCMV5 (QBIOgene Montreal, Canada) under the transcriptional control of a special cytomegalovirus (CMV) promoter–enhancer combination (CMV5) optimized for constitutive recombinant protein expression. The resulting shuttle plasmid, pAd-GFPCald (pJV1), was linearized with Cla I and co-transfected with an Ad5 viral DNA arm into 293 cells by calcium phosphate/DNA co-precipitation. The viral arm, QBI-viral DNA (QBIOgene, Montreal, Canada), was derived from Ad serotype 5, subtype dl327 with deletions at the E1a and E3 genes.

DNA precipitates of the pAd-GFPCald and QBI-viral DNA were exposed to the 293 cells for 12 hr washed exhaustively and allowed to recombine for 2 weeks. After recombination, harvested cells were lysed and their supernatant assayed for plaque purification by agar overlay (Borrás et al., 1996, 1998, 1999). Three GFP positive viral plaques were amplified and re-plated by agar overlay for a second plaque purification.

A purified viral stock of AdGFPCald was obtained by propagation in 293 cells and purified by double-banding in CsCl density gradients as previously described (Borrás et al., 1996, 1998, 1999). Purified viruses were titered by the agar overlay plaque assay in 293 cells. This viral stock (lot no. 010701) had a titer of 2.5×10^{10} particle forming units (pfu) per ml in a formulation vehicle of 0.01 M Tris pH 8, 0.01 M $MgCl_2$ and 10% glycerol.

Absence of contaminant wild type viruses in lot no. 010701 was tested by PCR amplification with E1A primers 5′-TCGAAGAGGTACTGGCTGAT-3′ and 5′-TGACAA-GACCTGCAACCGTG-3′.

Sequence confirmation of AdGFPCald was obtained by amplifying the expression cassette with pQBI-AdCM V5 flanking primers (606–634 and 815–788 nt in pQBI-AdCMV5, respectively) and fully sequencing the fragment in both directions with additional internal primers. No mismatches were found to referenced sequences with the exception of a potential change of an alanine to a valine at amino acid 68 of the caldesmon protein.

Adenovirus carrying the green fluorescent protein (AdGFP) was acquired from QBIOgen (Montreal, Canada) and grown

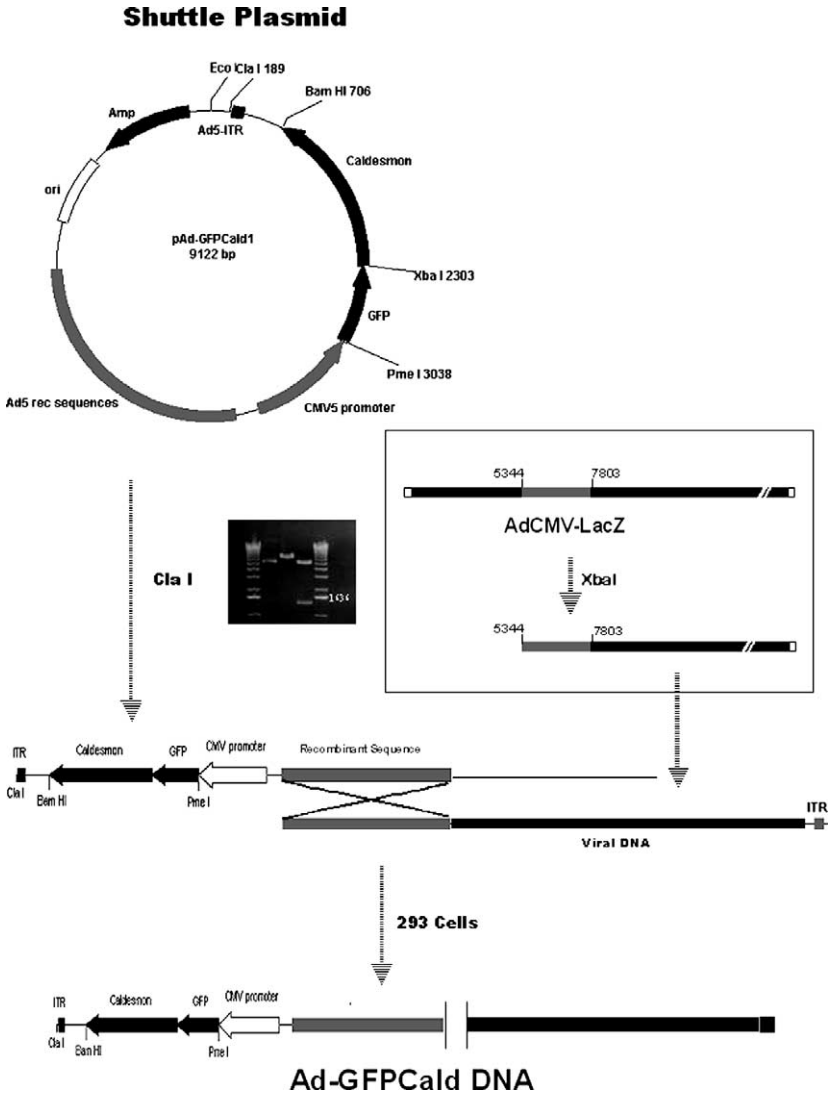

Fig. 1. Vector construction diagram. See Section 2 for further details.

and purified in our laboratories. It contains the same backbone and promoter as the AdGFPCald, i.e. it is derived from Ad5 serotype with deletions in the E1A and E3 regions and the transgene is driven by the CMV promoter–enhancer (Borrás et al., 2001).

2.2. HTM cell culture

Eyes from non-glaucomatous human donors were obtained within 48 hr of death from national eye banks (Lions Eye Bank of Oregon and National Disease Research Interchange) following signed consent of the patients' families. All procedures were in accordance with the Tenets of the Declaration of Helsinki. For isolation of HTM cells, (Comes et al., 2005) the TM from a single individual was isolated from surrounding tissue by making incisions both anterior and posterior to the meshwork and removing it using forceps. The tissue was then cut into small pieces, treated with 1 mg ml^{-1} collagenase in phosphate buffered saline (PBS) and incubated at 37 °C in a shaker water-bath for 1 hr. Incubation was followed by low speed centrifugation for 5 min. Pellets were resuspended in 4 ml of Improved Minimal Essential Medium (IMEM; Biofluids, Rockville, MD) supplemented with 20% fetal bovine serum (FBS) and 50 μg ml^{-1} gentamicin (GIBCO Invitrogen, Carlsbad, CA). Resuspended tissue was plated on a single, 2% gelatin-coated 35 mm dish and maintained in a 37 °C, 7% CO_2 incubator. Once confluent (2–3 weeks), cells were passed to a T-25 flask and labelled as passage 1. Subsequently, cells were passed 1:4 at confluency and maintained in the same medium with 10% FBS (complete IMEM). These primary, non-transformed cells subsist for 9–10 passages. Cell lines used here were HTM-29 (stillborn donor) and HTM-39 (17-year-old donor).

Cells were dissociated by trypsinization and replated either on Petri dishes with coverslips placed onto the bottom (for subsequent fixation and immunofluorescence staining). For the majority of the experiments the confluent culture of HTM cells was split 1:4 for replating. Twenty-four hours after replating,

the cells were infected with the AdGFPCald or AdGFP (10 pfu cell^{-1}) and examined 24 hr after transduction. At that time, about 90% of cells were positive for GFP-fluorescence. 50–60% of infected cells exhibited prominent morphological changes typical for caldesmon-transfected cells (Helfman et al., 1999).

2.3. Immunofluorescence microscopy

Cells were fixed and subjected to immunofluorescence staining of cytoskeletal proteins. Usually after brief rinsing in PBS at 37 °C cells were fixed by 3% paraformaldehyde in PBS for 20–30 min at the room temperature. After fixation cells were rinsed with PBS and permeabilized with 0.5% of Triton X-100 in PBS for 5 min. When a higher degree of permeabilization was required, the cells were first fixed with a mixture containing 0.1% Triton X-100 and 3% paraformaldehyde in PBS for 2–3 min and then post-fixed with 3% paraformaldehyde for 20 min. For actin staining, cells were subsequently incubated with 100 nM TRITC-phalloidin (Sigma, St Louis, MO); for antibody-staining, cells were incubated with primary antibodies diluted in PBS. Cells were then washed in PBS three times and incubated with the secondary, fluorochrome-conjugated antibodies. After three final washes the coverslips were mounted in Elvanol and the specimens were viewed and analyzed. For focal adhesions, monoclonal anti-human vinculin (Sigma) primary antibodies were used in this study.

Images were recorded on an Axiovert 100 TV inverted microscope (Zeiss, Oberkochen, Germany) equipped with a 100 W mercury lamp, a 100X/1.4 plan-Neofluar objective (Zeiss, Oberkochen, Germany), excitation and emission filter wheels, and a CCD camera (CH300/CE 350, Photometrics, Tucson, AZ) with KAF1400 CCD chip, controlled by a DeltaVision system (Applied Precision, Inc., Issaquah, WA).

2.4. Organ culture: caldesmon studies

Eyes from rhesus monkeys (*Macaca mulatta*) from the Wisconsin National Primate Research Center and cynomolgus monkeys (*Macaca fascicularis*) from Dr Kaufman's colony, that were being euthanized for other protocols, were obtained fresh and placed in organ culture usually less than 2 hr after enucleation. A monkey anterior segment organ culture system (see manuscript by Hu et al., in this issue) was used to test the effects of the caldesmon-expressing adenoviral vector on outflow facility using the two-level constant pressure perfusion technique (Bárány, 1964). Briefly, fluid flow from an external reservoir was measured at two different pressures 10 mmHg apart alternated every 4 min for approximately 1 hr. Outflow facility was calculated as the change in flow divided by the change in pressure and sequentially averaged. Media infusion continued at a constant rate of 2.5 μl min^{-1} when facility was not being measured. A total of 10 pairs of monkey anterior segments were studied in the caldesmon transduction experiments: six cynomolgus (*M. fascicularis*) and four rhesus (*M. mulatta*). Baseline outflow facility was measured after overnight equilibration. The eye with the lower baseline outflow facility was usually chosen to receive the AdCaldGFP to minimize the confounding effect of washout (see Section 4). This eye was injected via the inflow port with 20 μl containing 1.5×10^7 plaque forming units of AdGFPCald while the opposite eye received the same dose of AdGFP. In some of the initial pairs of segments, outflow facility was not measured daily since, expression was not expected to reach a maximum for several days based on in vitro cell studies (see manuscript by Grosheva et al. in this issue) and preliminary studies in monkey eyes in vivo injected with the same dose (Kaufman, unpublished data). Outflow facility was measured for up to 6 days. In the case of one pair in which the control eye was unusable, the control data was replaced with the average from control segments from two other pairs from the same species studied at the same time; therefore, the total number of segments was 19.

The effect of caldesmon over-expression on outflow facility was also studied in the human anterior segment organ culture system as previously described (Borrás et al., 1999; Vittitow et al., 2002) using the constant rate infusion method (Johnson and Tschumper, 1987). Anterior segments from six pairs of eyes were perfused at a constant rate of 2.5–3.5 μl min^{-1}. After 24 hr of equilibration, baseline outflow facility was determined. Then 20 μl containing 10^7 pfu of the AdGFPCald construct was injected through the cornea into one eye; viral vehicle was injected into the opposite eye. IOP was monitored continuously and outflow facility calculated every 3–6 hr for 66 hr.

2.5. GFP fluorescence and light microscopy in anterior segments

At the conclusion of the caldesmon outflow facility studies, all monkey eyes were perfused with 5 ml of 4% paraformaldehyde for 30 min, then cut into quadrants or eighths. One piece from each quadrant was then immersed in either 4% paraformaldehyde, Ito's fixative (Ito and Karnovsky, 1968) or graded concentrations of sucrose. Human segments were immersion fixed for 1 hr in 4% paraformaldehyde followed by sucrose immersion as described (Borrás et al., 2001). Segments in sucrose were then embedded in OCT compound and frozen sections cut and examined by fluorescence microscopy for GFP fluorescence in the outflow pathways.

For light microscopy, pieces from monkey anterior segments that were fixed in either 4% paraformaldehyde or Ito's were embedded in JB-4 solution (Polysciences, Inc., Warrington, PA), 4 μm sections were cut and mounted on glass slides, and then stained with Toluidine blue O (Polysciences, Inc., Warrington, PA). Pieces from human anterior segments were embedded in paraffin and sections stained with hematoxylin and eosin. The presence of TM cells, beams and the integrity of Schlemm's canal were assessed.

2.6. Analysis

Data are expressed as the mean ± SEM and were analyzed by the two-tailed paired *t*-test for ratios compared to 1.0. Treated

and control segments were compared to each other and after normalization for baseline differences.

3. Results

3.1. Focal adhesions in control HTM cells

Sparse or sub-confluent cultures of HTM cells were studied. Actin cables (known also as stress fibers) were prevalent actin structures in these cells. They formed one or few densely packed parallel arrays traversing through the entire cell and filling the whole cytoplasm (Fig. 2A).

Staining of the HTM cells with anti-vinculin antibodies was used to characterize the organization of the cell–matrix adhesions. The major type of adhesion structures in the HTM cells are 'classical' focal adhesions—elongated plaques with approximate width and length 0.5–1.0 and 2–5 μm, respectively—readily visualized by vinculin antibody staining (Fig. 2B). Focal adhesions are associated with the ends of actin-containing stress fibers (not shown). Focal adhesions are known to evolve from small dot-like focal complexes that continuously appear underneath the lamellipodial protrusions. In HTM cells, vinculin positive dot-like focal complexes can be observed in association with peripheral lamellipodia (not shown).

3.2. Effect of caldesmon over-expression on focal adhesions

Qualitatitive observation revealed no notable cytotoxicity. Infected cells reached confluency simultaneously with

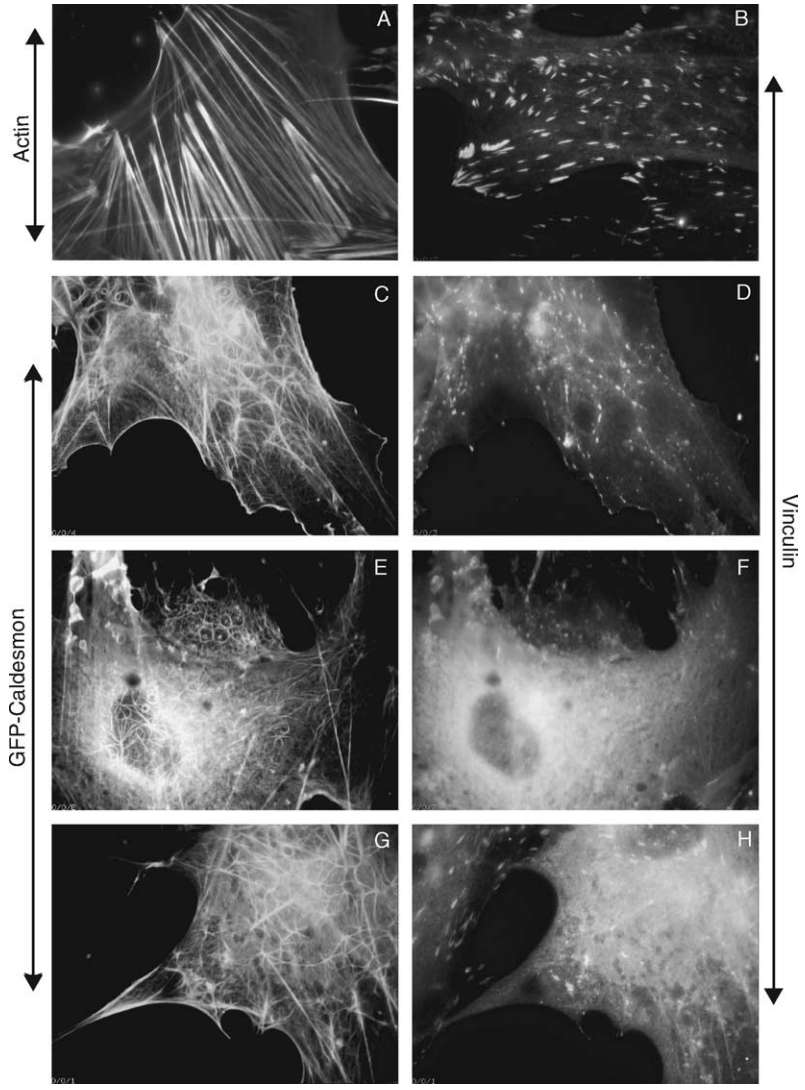

Fig. 2. Typical organization of the cytoskeleton in control HTM cells and effect of caldesmon over-expression on the focal adhesions. (A) Phalloidin staining reveals long, straight stress fibers. (B) Vinculin staining reveals numerous elongated focal adhesions. (C–H) three examples of HTM cells transduced with adenovirus encoding GFP-caldesmon. Distribution of GFP-caldesmon in individual cells are shown in C, E and G; distribution of vinculin in the same cells in D, F, and H, respectively. Caldesmon localized to actin-containing fibers dramatically alters their organization in the cell. Vinculin, a marker of cell–matrix adhesions, is diffusely distributed in the caldesmon-over-expressing cells and does not reveal prominent focal adhesions (D, F, H) (compare with B). Small, residual patches are sometimes seen at the cell periphery and in association with remaining actin fibers D. Non-transduced cell in the same culture contain well-developed focal adhesions (a fragment of such a cell is seen in the left upper corner of the photograph H).

non-treated cells, indicating that proliferation was not affected. Approximately 90% of cells appeared to express GFP/Caldesmon.

GFP-caldesmon expressed in HTM cells decorates all actin-containing structures, including stress fibers and other actin filament bundles, ruffles, lamellipodia, etc. so there is always complete co-localization of GFP-caldesmon and F-actin visualized by phalloidin staining (not shown). At the same time, the actin cytoskeleton in the cells expressing caldesmon underwent apparent reorganization described in detail in the accompanying paper by Grosheva et al. Three typical examples of transduced cells are presented in Fig. 2C–H. GFP-caldesmon-labelled actin cytoskeleton demonstrates different degrees of disorganization, from relatively mild in C to more severe in E and G.

In cells with disrupted stress fibers, vinculin-containing focal adhesions were also disrupted and vinculin was diffusely distributed in the cytoplasm (Fig. 2F and H). However in the cells or in the cell regions where short stress fibers were still preserved, vinculin-containing focal adhesions were also detected (Fig. 2D), albeit smaller and less prominent than in control cells (Fig. 2B).

3.3. Effect of caldesmon over-expression on outflow facility

In organ-cultured anterior segments, baseline outflow facility (μl min^{-1} $mmHg^{-1}$) averaged (mean ± SEM): human, 0.19 ± 0.03 ($n = 12$ (six pairs)); monkey, 0.36 ± 0.02 ($n = 19$ (10 pairs, as explained in Section 2)).

In human segments, the average IOP began to decrease in AdGFPCald segments within 24–36 hr after the injection. Outflow facility was increased in AdGFPCald transduced segments by 43 ± 21% ($p \leq 0.11$, $n = 6$) at 66 hr compared to baseline and corrected for the changes in outflow of the contralateral vehicle-treated segment. Three pairs showed a strong response at 66 hr while the other three pairs showed virtually no response at that time point (Fig. 3A). A sample tracing for one pair of segments is shown in Fig. 3B.

In pairs of monkey anterior segments, the segment with the lower baseline outflow facility was chosen to receive the AdGFPCald while the opposite segment received the AdGFP. Baseline outflow facility was significantly less in to-be-treated compared to to-be-control segments (Table 1). Following treatment, an outflow facility increase was detected as early as 1 day after transduction, with the maximum outflow facility increase occurring from 1 to 6 days after transduction (Fig. 4). The mean maximum outflow facility increase in pairs of AdGFPCald vs AdGFP segments corrected for baseline was 66 ± 18%, ($p < 0.01$, $n = 10$, day 1–6). However, given the lower starting baseline outflow facility of AdGFPCald segments, this ratio would bias the results in favour of the caldesmon. Comparison of AdGFPCald to AdGFP without correction for baseline would bias the data against detecting an outflow facility response to caldesmon.

On days 2 or 3 after transduction, which corresponds to the time of the human segment data, 10 monkey pairs of segments showed a 35 ± 18% ($p < 0.2$, $n = 10$) increase in outflow facility

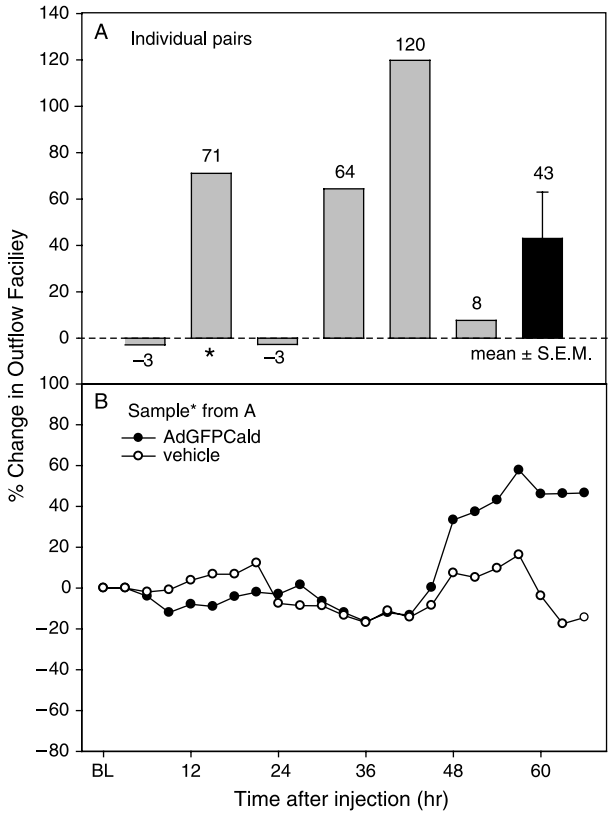

Fig. 3. Outflow facility in human organ-cultured anterior segments after injection of AdGFPCald or vehicle. (A) Percent change in outflow facility at 66 h post-injection in pairs of segments: AdGFPCald/baseline compared to vehicle/baseline. (B) Percent change in outflow facility compared to baseline for each segment of the pair indicated by * in A: AdGFPCald/baseline and vehicle/baseline.

Table 1
Effect of caldesmon gene therapy on outflow facility in human and monkey organ-cultured anterior segments

	Outflow facility (μl min^{-1} $mmHg^{-1}$)			
	$N=$	AdGFPCald	Veh or AdGFP	AdGFPCald/ Veh or AdGFP
Human				
Baseline	6	0.18 ± 0.04	0.20 ± 0.05	0.97 ± 0.09
Rx	6	0.25 ± 0.05	0.21 ± 0.05	1.42 ± 0.28
Rx/BL	6	1.49 ± 0.25	1.04 ± 0.07	1.43 ± 0.20
Monkey				
Baseline	10 (d1–6)	0.32 ± 0.03	0.40 ± 0.03	0.82 ± 0.06*
	10 (d2–3)	0.62 ± 0.10	0.59 ± 0.05	1.08 ± 0.15
Rx	10 (d1–6)	0.83 ± 0.17	0.60 ± 0.06	1.35 ± 0.17
	10 (d2–3)			
Rx/BL	10 (d1–6)	2.43 ± 0.35**	1.53 ± 0.17*	1.66 ± 0.18***
	10 (d2–3)	1.90 ± 0.22**	1.52 ± 0.14***	1.35 ± 0.18
Combined data (*Monkey*, *day 2–3 corresponding to human data timing*)				
Baseline	16	0.27 ± 0.03	0.33 ± 0.04	0.88 ± 0.05
Rx	16	0.48 ± 0.08	0.45 ± 0.06	1.21 ± .014
Rx/BL	16	1.75 ± 0.17†	1.34 ± 0.11***	1.38 ± 0.13*

Data are mean ± SEM Ad, adenoviral vector; GFP, green fluorescent protein; Cald, caldesmon; Rx, treated; *N*, 6 (human data at 66 hr post-injection); *n*, 10 (monkey data, maximum response in days 1–6 or days 2–3); *n*, 16 (human and monkey data (monkey data from day 2 to 3 after transduction similar to timing of human data). Ratio significantly different from 1.0 by the two-tailed paired *t*-test; *$p < 0.05$, **$p < 0.005$, ***$p < 0.01$, †$p < 0.001$.

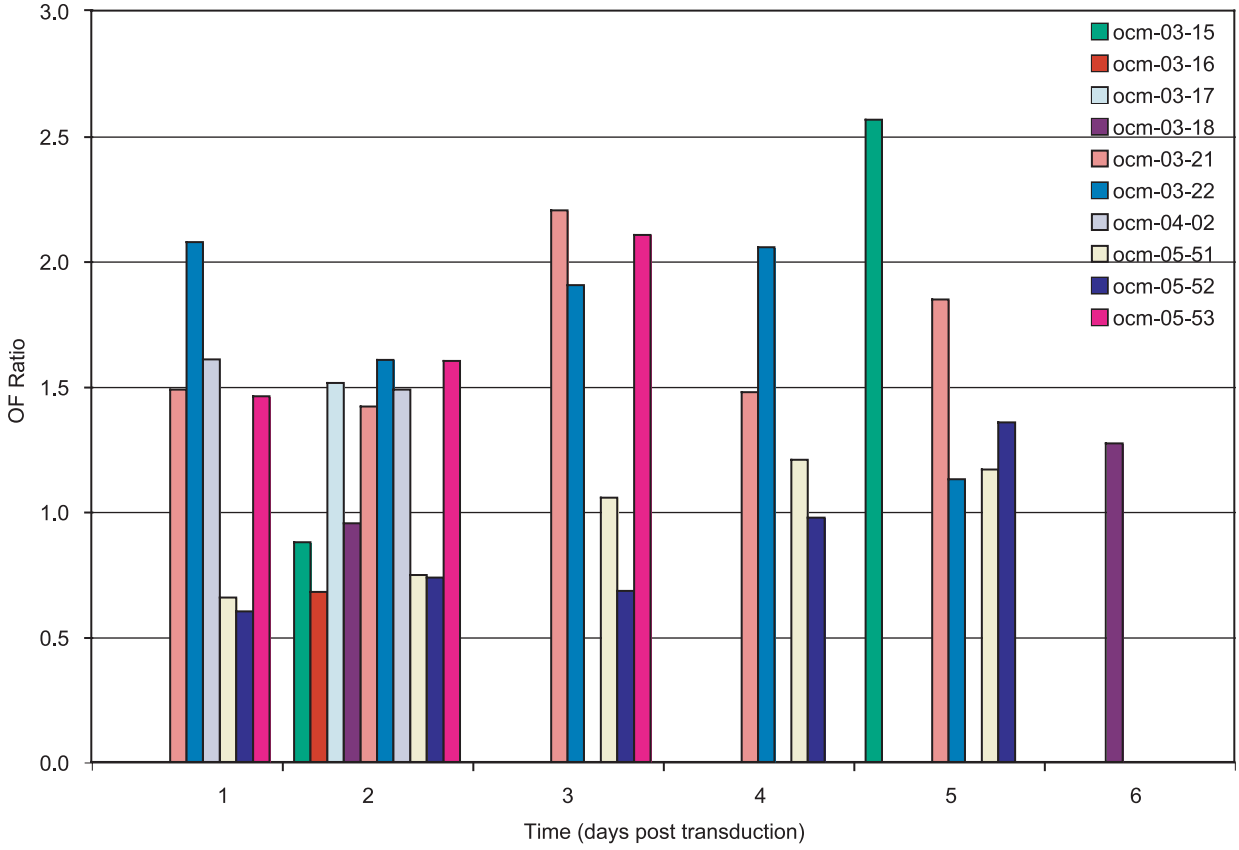

Fig. 4. Outflow facility in monkey organ-cultured anterior segments. Ratio of AdGFPCald/AdGFP corrected for baseline for each day of measurements after transduction. Each colour represents a pair of segments. Outflow facility was not measured in every pair each day. OF, outflow facility.

in AdGFPCald compared to AdGFP segments corrected for baseline. This result includes five pairs that did not respond at this time (Fig. 4), comparable to the percentage of human segments that did not respond in this time period (Fig. 3). The combined human (66 hr) and monkey (2–3 days) data showed a significant increase in outflow facility in caldesmon transduced segments of $38 \pm 13\%$ ($p < 0.05$, $n = 16$) (Table 1) when compared to the contralateral control and corrected for baseline.

3.4. GFP fluorescence and light microscopy of anterior segments

Fluorescence was present in the TM of AdGFPCald segments from human eyes (Fig. 5A, B) and in both pairs (AdGFPCald and AdGFP) of monkey segments (Fig. 6A, D). In human segments, some fluorescence was also visible in the corneal endothelium. In monkey segments, fluorescence may also have been associated with the cornea and the remnant of the ciliary body although the morphology of the frozen sections was not well preserved.

In human anterior segments, light microscopy showed that the TM of AdGFPCald treated segments (Fig. 5C) had a less dense appearance, especially in the juxtacanalicular area compared to the contralateral vehicle control (Fig. 5D). TM cells also appeared to be more rounded. Schlemm's canal seemed to be intact.

Light microscopic examination of monkey anterior segments revealed that AdGFP controls had intact Schlemm's canal and organized trabecular beams, and exhibited a high degree of cellularity throughout the TM and Schlemm's canal (Fig. 6E). Segments transduced with AdGFPCald for 5 days (Fig. 6B, C), showed some disruption of trabecular beams and cells appeared to be rounded up. Schlemm's canal seemed to be intact. Morphological examination of the juxtacanalicular area was inconclusive and requires additional studies at the electron microscopic level.

4. Discussion

It has been shown previously that caldesmon over-expression leads to disruption of stress fibers and focal adhesions in cultured fibroblasts (Helfman et al., 1999). In the current study, we showed that a similar effect is also observed in HTM cells. These cells have a very well developed actin cytoskeleton system, and demonstrate more complex responses to caldesmon than fibroblasts (See accompanying paper by Grosheva et al.). However, disappearance of stress fibers and associated vinculin-positive focal adhesions is typical for both systems. Cells positive for GFP-fluorescence as a rule exhibited certain degrees of actin reorganization and apparent reduction in the number

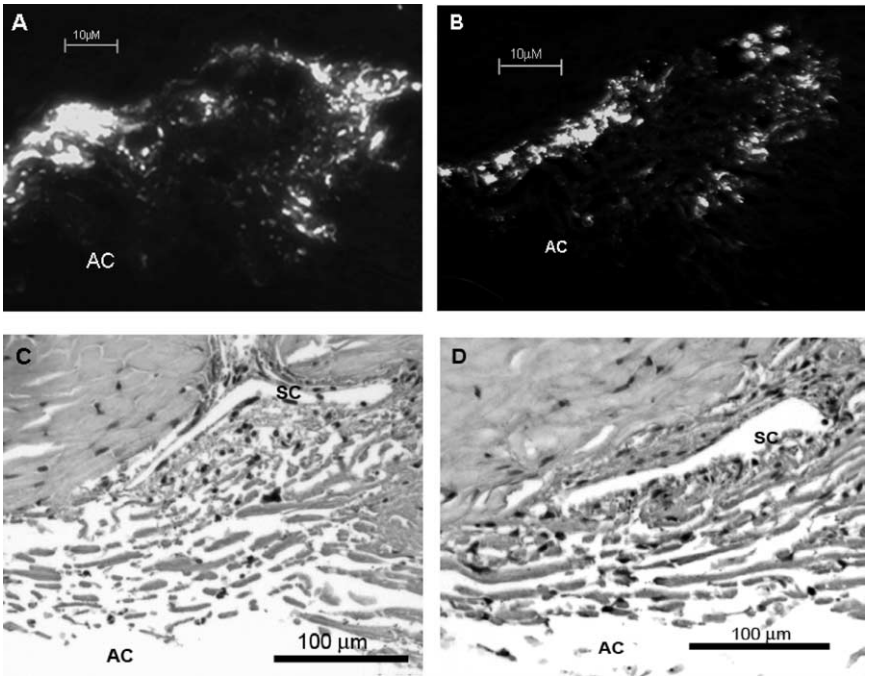

Fig. 5. Green fluorescence protein (GFP) expression and light microscopy of a human organ-cultured anterior segment treated with 10^7 pfu of AdGFPCald. (A, B) GFP expression in quadrants 180° apart in the same AdGFPCald treated segment. (C, D) Hematoxylin and eosin staining of the TM of the AdGFPCald treated segment C and D the contralateral vehicle treated segment. The TM of the AdGFPCald treated segment appears less dense in the juxtacanalicular area and the TM cells appear more rounded than in the vehicle treated segment. AC, anterior chamber; SC, Schlemm's canal.

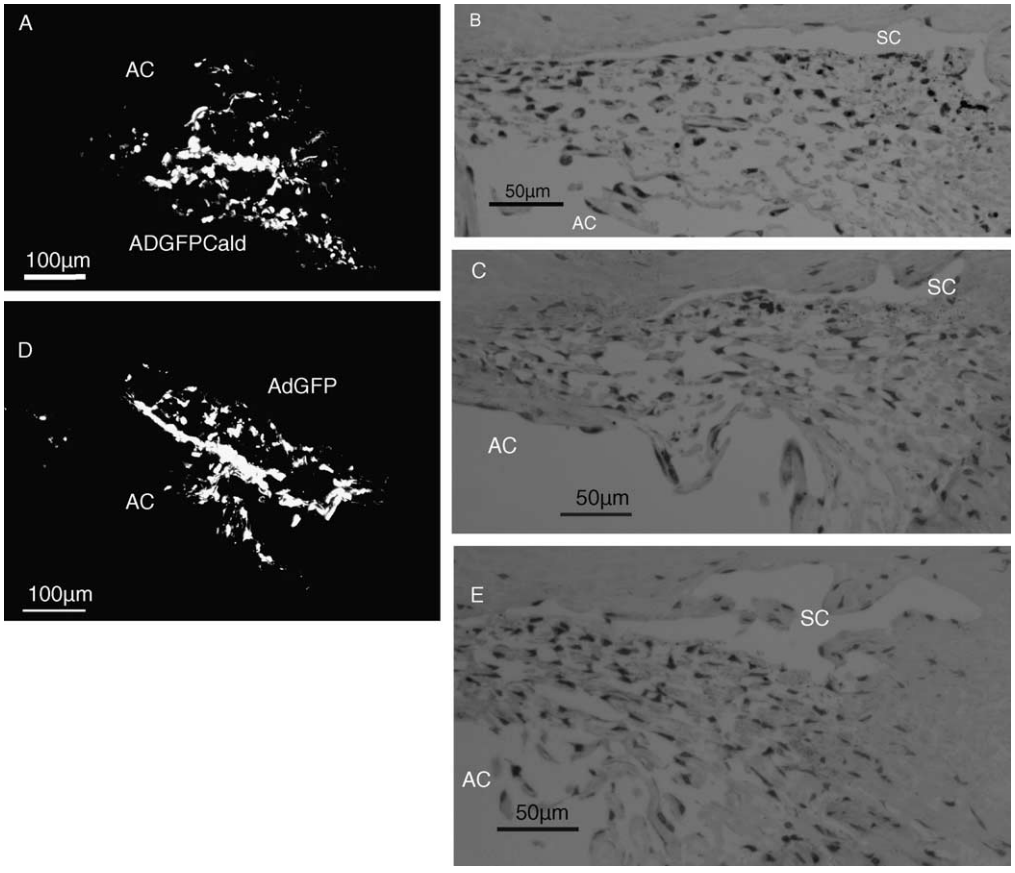

Fig. 6. GFP fluorescence and light microscopy in pairs of monkey organ-cultured anterior segments, 5 days after transduction with AdGFPCald to one segment, AdGFP to the contralateral segment. (A, D) GFP fluorescence demonstrates that efficient transduction of the TM occurs when the tissue is in its normal configuration. (B, C, E) Toluidine blue staining reveals some disruption of the TM 5 days after transduction with AdGFPCald B, C compared to AdGFP alone E. B, C are different quadrants from the same segment. Segments are from pair ocm-05-52 (see Fig. 4 for corresponding outflow facility results). AC, anterior chamber; SC, Schlemm's canal.

and size of focal adhesions. In about 40–50% of transduced cells, changes in the actin cytoskeleton were severe and were accompanied by complete loss of focal adhesions.

Over-expression of caldesmon in organ-cultured anterior segments increased outflow facility. The response in human anterior segments may have been greater if the experiment were carried out for longer periods of time as was done with the monkey anterior segments. A complete dose–response relationship was not established; therefore, the caldesmon dose may not have been optimal for inducing the maximum outflow facility response. The dose selected for use in organ culture was similar to that found to produce minimal inflammation when injected into the monkey eye in vivo (Kaufman, unpublished data). Also, the number of particle forming units per TM cell used in the organ-cultured anterior segments was similar to that used with the cultured cells (10 pfu cell^{-1}), assuming there are approximately 1.2×10^6 TM cells in human TM (Grierson and Howes, 1987). Presumably the monkey TM (Gabelt et al., 2003) would have proportionally less TM cells compared to the human eye based on relative size of the eyes. Therefore, the particle forming units per cell may have been slightly higher in the monkey segments. However, all of the viral particles administered did not necessarily go only to the TM; therefore, the effective dose may have been less than that administered to HTM cells in vitro. The variation in the degree of actin reorganization observed in HTM cells in culture as a result of caldesmon over-expression presumably also occurs in the TM of the organ cultured anterior segments. Interestingly, the results are quite similar since approximately 50% of HTM cells in culture showed severe changes and nearly the same percentage of organ-cultured anterior segments demonstrated an outflow facility response.

The magnitude of the outflow facility increase resulting from caldesmon over-expression in monkey organ-cultured anterior segments in the current study is nearly identical to that found with 300 μM H-7 treatment in this system (see manuscript by Hu, this issue) and to 100 μM H-7 (Tian et al., 1998) or 0.5 μM latrunculin-A (Peterson et al., 1999) in monkey eyes in vivo. More detailed morphological analysis is needed to determine whether structural effects such as cell relaxation, expansion of the juxtacanalicular region, dilation of Schlemm's canal and luminal protrusion of the inner wall similar to those induced by to H-7 or latrunculin-A or -B are produced (Sabanay et al., 2000; in press). Transduction with AdGFPCald in HTM cells disrupts focal adhesions by altering cell–cell junctions (Vittitow et al., 2004) similar to what has been observed in HTM cells treated with latrunculin-A (Cai et al., 2000).

The presence of fluorescence in the TM in both the AdGFPCald and AdGFP pairs of segments of monkey eyes and in the AdGFPCald segment of human eyes indicates that efficient transduction can occur when the TM tissue is in its original configuration, much as it would be in vivo without the cells dissociated and spread out as they are in tissue culture. Future studies incorporating TM specific promoters (Gonzalez et al., 2004; Liton et al., 2005) should permit even better localization of expression to the TM.

Gene therapy to inhibit the Rho-mediated signalling pathway for actomyosin contractility via over-expression of the bacterial exoenzyme C3 also disrupts the HTM cell cytoskeleton and increases outflow facility in monkey anterior segment organ culture (Liu et al., 2005). Similarly, over-expression of a dominant negative RhoA disrupted the cytoskeleton and increased outflow facility in human organ-cultured anterior segments (Vittitow et al., 2002). Caldesmon over-expression prevents focal adhesion and stress fiber formation even if the cells express constitutively active Rho, showing that caldesmon is operating downstream from the Rho signalling pathway (Helfman et al., 1999). It is possible that gene therapy combining caldesmon and C3 or dominant negative RhoA could lead to even greater outflow facility enhancement.

For the monkey organ culture experiments, we selected the segment with the lower baseline outflow facility to receive the AdGFPCald-expressing adenoviral vector. This selection favourably biased the detection of an increased response when compared to baseline (regression to the mean). Comparison of the post-treatment outflow facilities in opposite eyes without correction for baseline, biased the result against detection of an effect, since the baseline outflow facility was lower to start with in the AdGFPCald-treated eyes. Random assignment of the eyes to receive the AdGFPCald would have minimized both of these biases and, retrospectively, would have been preferable.

Combining the human and monkey data assumes that they respond similarly. Using the 2–3 days data from the monkey studies for the combined analysis was necessary statistically since, that was the timing used in the human studies. However, the maximum response may not have been attained in the monkey segments (compare 1–6 and 2–3 days Rx line in Table 1). Continuing the measurements for additional days in human and monkeys segments would likely have increased the magnitude of the outflow facility response to caldesmon over-expression. Therefore, additional experiments in both human and monkey segments are warranted.

The current study is the first demonstration that over-expression of an endogenous protein (caldesmon) via gene transfer can be used to modulate outflow facility in the primate TM in vitro. Advances in vector technology for the anterior segment of the eye will soon make the study of caldesmon over-expression possible in vivo where long-term effects may be assessed. Caldesmon ocular gene therapy could potentially be used to reduce IOP in glaucoma.

Acknowledgements

This research was supported by NEI EY02698 (PLK), EY011906 and EY13126 (TB), RPB (PLK); NEI P30 EY016665 (PLK, Core Grant for Vision Research); P51 RR00167 (Wisconsin National Primate Research Center), Ocular Physiology Research and Education Foundation (PLK), NIH EY07119 (training grant for the Department of Biostatistics and Medical Informatics at the University of Wisconsin)

The authors thank Mark Filla, PhD for assistance with the fluorescence microscopy of monkey anterior segments and Timothy Grant, MS for statistical analysis consultation.

Commercial Relationships: TB (patent, Duke University), PLK (patent, University of Wisconsin), BG and AB (patent, Weizmann Institute of Science).

References

Bahler, C.K., Hann, C.R., Fautsch, M.P., Johnson, D.H., 2004. Pharmacologic disruption of Schlemm's canal cells and outflow facility in anterior segments of human eyes. Invest. Ophthalmol. Vis. Sci. 45, 2246–2254.

Bárány, E.H., 1964. Simultaneous measurements of changing intraocular pressure and outflow facility in the vervet monkey by constant pressure infusion. Invest. Ophthalmol. 3, 135–143.

Bershadsky, A., Chausovsky, A., Becker, E., Lyubimova, A., Geiger, B., 1996. Involvement of microtubules in the control of adhesion-dependent signal transduction. Curr. Biol. 6, 1279–1289.

Borrás, T., Tamm, E., Zigler Jr., J.S., 1996. Ocular adenovirus gene transfer varies in efficiency and inflammatory response. Invest. Ophthalmol. Vis. Sci. 37, 1282–1293.

Borrás, T., Masumoto, Y., Epstein, D.L., Johnson, D.H., 1998. Gene transfer to the human trabecular meshwork by anterior segment perfusion. Invest. Ophthalmol. Vis. Sci. 39, 1503–1507.

Borrás, T., Rowlette, L.L., Erzurum, S.C., Epstein, D.L., 1999. Adenoviral reporter gene transfer to the human trabecular meshwork does not alter aqueous humor outflow. Relevance for potential gene therapy of glaucoma. Gene Ther. 6, 515–524.

Borrás, T., Gabelt, B.T., Klintworth, G.K., Peterson, J.C., Kaufman, P.L., 2001. Non-invasive observation of repeated adenoviral GFP gene delivery to the anterior segment of the monkey eye in vivo. J. Gene Med. 3, 437–449.

Cai, S., Liu, X., Glasser, A., Volberg, T., Filla, M., Geiger, B., Kaufman, P.L., 2000. Effect of latrunculin-A on morphology and actin-associated adhesions of cultured human trabecular meshwork cells. Mol. Vis. 6, 132–143.

Chalovich, J.M., Sen, A., Resetar, A., Leinweber, B., Fredricksen, R.S., Lu, F., Chen, Y.D., 1998. Caldesmon: binding to actin and myosin and effects on elementary steps in the ATPase cycle. Acta Physiol. Scand. 164, 427–435.

Chrzanowska-Wodnicka, M., Burridge, K., 1996. Rho-stimulated contractility drives the formation of stress fibers and focal adhesions. J. Cell Biol. 133, 1403–1415.

Comes, N., Gasuli, X., Gual, A., Borras, T., 2005. Differential expression of the human chloride channel genes in the trabecular meshwork under stress conditions. Exp. Eye Res. 80, 801–813.

Epstein, D.L., Rowlette, L.-L., Roberts, B.C., 1999. Acto-myosin drug effects and aqueous outflow function. Invest. Ophthalmol. Vis. Sci. 40, 74–81.

Gabelt, B.T., Gottanka, J., Lütjen-Drecoll, E., Kaufman, P.L., 2003. Aqueous humor dynamics and trabecular meshwork and anterior ciliary muscle morphologic changes with age in rhesus monkeys. Invest. Ophthalmol. Vis. Sci. 44, 2118–2125.

Goldberg, I., 1999. Compliance with medical therapy in chronic glaucoma. In: Gramer, E., Grehn, F. (Eds.), Pathogenesis and Risk Factors of Glaucoma. Springer, Berlin, pp. 25–33 (Chapter 4).

Gonzalez, P., Caballero, M., Liton, P.B., Stamer, W.D., Epstein, D.L., 2004. Expression analysis of the matrix GLA protein and VE-cadherin gene promotoers in the outflow pathway. Invest. Ophthalmol. Vis. Sci. 45, 1389–1395.

Grierson, I., Howes, R.C., 1987. Age-related depletion of the cell population in the human trabecular meshwork. Eye 1, 204–210.

Helfman, D.M., Lemy, E.T., Berthier, C., Shtutman, M., Riveline, D., Grosheva, I., Lachish-Zalait, A., Elbaum, M., Bershadsky, A.D., 1999. Caldesmon inhibits nonmuscle cell contractility and interferes with the formation of focal adhesions. Mol. Biol. Cell 10, 3097–3112.

Honjo, M., Tankhara, H., Inatani, M., Kido, N., Sawamura, T., Yue, B.Y.J.T., Narumiya, S., Honda, Y., 2001. Effects of rho-associated protein kinase inhibitor Y-27632 on intraocular pressure and outflow facility. Invest. Ophthalmol. Vis. Sci. 42, 137–144.

Huber, P.A., 1997. Caldesmon. Int. J. Biochem. Cell Biol. 29, 1047–1051.

Ito, S., Karnovsky, M.J., 1968. Formaldehyde-glutaraldehyde fixatives containing trinitro compounds. J. Cell Biol. 39, 168a–169a (Abs nr 418).

Johnson, D.H., Tschumper, R.C., 1987. Human trabecular meshwork organ culture: a new model. Invest. Ophthalmol. Vis. Sci. 28, 945–953.

Kaufman, P.L., Tian, B., Gabelt, B.T., Liu, X., 2000. Outflow enhancing drugs and gene therapy in glaucoma. In: Weinreb, R., Krieglstein, G., Kitazawa, Y. (Eds.), Glaucoma in the 21st Century. Harcourt/Mosby, London, pp. 117–128 (Chapter 17).

Liton, P.B., Liu, X., Stamer, W.D., Challa, P., Epstein, D.L., Gonzalez, P., 2005. Specific targeting of gene expression to a subset of human trabecular meshwork cells using the chitinase 3-like 1 promoter. Invest. Ophthalmol. Vis. Sci. 46, 183–190.

Liu, X., Hu, Y., Filla, M.S., Gabelt, B.T., Peters, D.M., Brandt, C.R., Kaufman, P.L., 2005. The effects of C3 transgene expression on actin and cellular adhesions in cultured HTM cells and on outflow facility in organ cultured monkey eyes. Mol. Vis. 11, 1112–1121.

Marston, S., Burton, D., Copeland, O., Fraser, I., Gao, Y., Hodgkinson, J., Huber, P., Levine, B., El-Mezgueidi, M., Notarianni, G., 1998. Structural interactions between actin, tropomyosin, caldesmon and calcium binding protein and the regulation of smooth muscle thin filaments. Acta Physiol. Scand. 164, 401–414.

Matsumura, F., Yamashiro, S., 1993. Caldesmon. Curr. Opin. Cell Biol. 5, 70–76.

Pelham, R.J., Wang, Y.-L., 1997. Cell locomotion and focal adhesions are regulated by substrate flexibility. Proc. Natl Acad. Sci. USA 94, 13661–13665.

Peterson, J.A., Tian, B., Bershadsky, A.D., Volberg, T., Gangnon, R.E., Spector, I., Geiger, B., Kaufman, P.L., 1999. Latrunculin-A increases outflow facility in the monkey. Invest. Ophthalmol. Vis. Sci. 40, 931–941.

Rao, P.V., Deng, P.-F., Kumar, J., Epstein, D.L., 2001. Modulation of aqueous humor outflow facility by the rho kinase-specific inhibitor Y-27632. Invest. Ophthalmol. Vis. Sci. 42, 1029–1037.

Ritch, R., Shields, M.B., Krupin, T., 1996. Chronic open-angle glaucoma: treatment overview. In: Ritch, R., Shields, M.B., Krupin, T. (Eds.), The Glaucomas, second ed. Mosby, St Louis, MO, pp. 1507–1519 (Chapter 73).

Riveline, D., Zamir, E., Balaban, N.Q., Schwarz, U.S., Ishizaki, T., Marumiya, S., Kam, Z., Geiger, B., Bershadsky, A.D., 2001. Focal contacts as mechanosensors: externally applied local mechanical force induces growth of focal contacts by an mDia1-dependent and ROCK-independent mechanism. J. Cell Biol. 153, 1175–1186.

Sabanay, I., Gabelt, B.T., Tian, B., Kaufman, P.L., Geiger, B., 2000. H-7 effects on structure and fluid conductance of monkey trabecular meshwork. Arch. Ophthalmol. 118, 955–962.

Sabanay, I., Tian, B., Gabelt, B.T., Geiger, B., Kaufman, P.L., 2004. Functional and structural reversibility of H-7 effects on the conventional aqueous outflow pathway in monkeys. Exp. Eye Res. 78, 137–150.

Sabanay, I., Tian, B., Gabelt, B.T., Geiger, B., Kaufman, P.L., in press. Latrunculin B effects on trabecular meshwork and corneal endothelium structure in the monkey eye. Exp. Eye Res.

Tian, B., Kaufman, P.L., Volber, T., Gabelt, B.T., Geiger, B., 1998. H-7 disrupts the actin cytoskeleton and increases outflow facility. Arch. Opthalmol. 116, 633–643.

Tian, B., Brumback, L.C., Kaufman, P.L., 2000. ML-7, chelerythrine and phorbol ester increase outflow facility in the monkey eye. Exp. Eye Res. 71, 551–566.

Tian, B., Wang, R.-F., Podos, S.M., Kaufman, P.L., 2004. Effects of topical H-7 on outflow facility, intraocular pressure and corneal thickness in monkeys. Arch. Ophthalmol. 122, 1171–1177.

Vittitow, J.L., Garg, R., Rowlette, L.L., Epstein, D.L., O'Brien, E.T., Borrás, T., 2002. Gene transfer of dominant-negative RhoA increases outflow facility in perfused human anterior segment cultures. Mol. Vis. 8, 32–44.

Vittitow, J.L., Grosheva, I., Bershadsky, A.D., Geiger, B., Kaufman, P.L., Borrás, T., 2004. Effect of rat non-muscle caldesmon overexpression on the cytoskeleton of human trabecular meshwork cells. Invest. Ophthalmol. Vis. Sci. 45 (Abs nr 4386).

Volberg, T., Geiger, B., Citi, S., Bershadsky, A.D., 1994. Effect of protein kinase inhibitor H-7 on the contractility, integrity and membrane anchorage of the microfilament system. Cell Motil. Cytoskeleton 29, 321–338.